

## Temperature dependence of the structure factor in Nb-Ni glasses

Soumen Basak, Roy Clarke, and S. R. Nagel

*Department of Physics, The University of Chicago, Chicago, Illinois 60637  
and The James Franck Institute, The University of Chicago, Chicago, Illinois 60637*

(Received 26 December 1978)

Using the results of x-ray scattering experiments, the structure factor  $S(k)$ , the radial distribution function, and the coordination number have been determined at room temperature for two Nb-Ni glass samples (of composition  $\text{Nb}_{0.4}\text{Ni}_{0.6}$  and  $\text{Nb}_{0.5}\text{Ni}_{0.5}$ ). Furthermore, the height of the first peak in the structure factor,  $S(k_p)$ , has been measured as a function of temperature for these two samples in the range 4–675 K.  $S(k_p)$  remains approximately constant from 4 to  $\sim 100$  K, after which it decreases linearly with increasing temperature until the glass crystallizes at  $\sim 675$  K. This behavior is in excellent agreement with a recent calculation which expresses the temperature dependence of  $S(k)$  of an amorphous metal in terms of the Debye-Waller factor. According to the Ziman theory for the resistivity of amorphous metals, a decrease of  $S(k_p)$  with increasing temperature may lead to a negative temperature coefficient of resistivity as has been observed in these glasses. The observed change of  $S(k_p)$  is large enough to account for the observed change in resistivity at room temperature and above. Possible reasons for the discrepancy between the Ziman theory and the structure-factor data below room temperature are discussed.

### I. INTRODUCTION

Metallic glasses are amorphous alloys of metals, with either other metals or with metalloids, which are prepared by rapid quenching of the melt to an amorphous solid. These materials often exhibit anomalous transport properties; for example, the temperature coefficient of resistivity  $\beta \equiv (1/\rho)d\rho/dT$  is negative in many of these glassy alloys,<sup>1</sup> whereas it is large and positive in most normal metals. Also, the thermoelectric power is positive in many of these glasses,<sup>2,3</sup> instead of negative, as simple theories would suggest. Various attempts have been made to explain these phenomena. One model<sup>4–6</sup> which has been proposed is based on the tunneling of atoms in a disordered solid between two sides of a double potential well and predicts a negative value of  $\beta$  for a metallic glass. This model was originally proposed to explain the linear term in the low-temperature specific heat observed in insulating glasses.<sup>7</sup> The concentration of such tunneling levels in a glass is expected to be dependent on the alloy composition,<sup>5</sup> whereas a series of experiments on Nb-Ni glasses<sup>8</sup> has shown that the low-temperature behavior of  $\rho$  is essentially independent of composition. Also thermoelectric-power measurements<sup>2</sup> on a Be-Ti-Zr glass do not appear to be consistent with this model. A second theory<sup>9,10</sup> relates the resistivity behavior in glasses containing transition metals to the scattering of valence  $s$  electrons into unoccupied  $d$ -band states of the transition metal. This model is also inconsistent with the thermoelectric-power data mentioned above, since the sign of the thermoelectric power should change upon going from a nearly empty  $d$  band to a nearly filled  $d$  band. This has not been

observed experimentally. A third alternative deals with the normal electron-phonon contribution to the resistivity as modified by the absence of periodic order in a glass. This theory was originally proposed by Ziman<sup>11</sup> to explain the negative values of  $\beta$  observed in such divalent liquid metals as Zn. Subsequently, it was extended and modified to treat liquid transition metals<sup>12</sup> and metallic glasses.<sup>3</sup> For a transition-metal system it gives the following expression for the resistivity<sup>12</sup>:

$$\rho = (30\pi^2\hbar^3/m e^2 k_F^2 E_F \Omega) \sin^2[\eta_2(E_F)] S(2k_F), \quad (1.1)$$

where  $k_F$  and  $E_F$  are the Fermi wave vector and energy, respectively, and  $\Omega$  is the atomic volume,  $\eta_2(E_F)$  is the  $d$ -wave phase shift describing the scattering of the conduction electrons, of energy  $E_F$ , by the ion cores which are assumed to carry a muffin-tin potential. Information about the structure of the material enters the expression through the structure factor  $S(k)$ .

According to Eq. (1.1), the temperature dependence of  $\rho$  is determined by that of  $S(2k_F)$  which has recently been calculated for an amorphous metal.<sup>13</sup> The result for the temperature dependence of the static structure factor is

$$S_T(k) = 1 + [S_0(k) - 1] e^{-2[W(T) - W(0)]}, \quad (1.2)$$

where  $S_0(k)$  is the structure factor at  $T=0$  K and  $e^{-2W(T)}$  is the Debye-Waller factor at temperature  $T$ . At low  $T$  the resistivity will vary slightly slower than the static structure factor.<sup>14</sup>

A different approach than that employed here was described some years ago in an x-ray study<sup>15</sup> of amorphous selenium at two temperatures. In

that work the pair distribution function  $g(r)$  was fit to the data by using a different coupling coefficient for each separate peak. Using 18 free parameters, the authors fit the temperature dependence of their structure out to 7.6 Å. In the case of selenium this procedure is perhaps the best alternative because the molecular structure of this solid is quite complex and different shells of neighbors will have quite different vibrational amplitudes. For selenium the large- $r$  behavior will determine the low wave-vector peaks in  $S(k)$ . In our case the situation is quite different from that in selenium and in many ways more simple. For the metallic glasses the Ehrenfest relation is quite well satisfied, as we will show later in this paper. This implies that not only the large- $r$  correlations contribute to the first peak in  $S(k)$ , but that the nearest-neighbor distances are reflected in this peak as well. Since for the metallic and other close-packed glasses a large part of  $r$  space is reflected in each peak in  $S(k)$ , it becomes much less important to invoke different coupling constants for each shell of neighbors. In effect, we go over to a case in which each peak in  $S(k)$  is affected by an averaged Debye-Waller factor. Thus we find that we need only one adjustable parameter to describe the temperature dependence of  $S(k)$ , instead of the many necessary for selenium. As we shall see from the present x-ray study, this simple model is in excellent agreement with our data. By measuring the temperature dependence of more than one peak in  $S(k)$  for a metallic glass, we are able to show that the approximations made in using one average Debye temperature for all peaks are physically justified.

In this paper we report the result of measurements of the temperature dependence of  $S(k)$  of  $\text{Nb}_x\text{Ni}_{1-x}$  glasses carried out over a wide range of temperatures (4–675 K) and for samples whose compositions span much of the glass-formation range of this alloy ( $x=0.4$  and  $0.5$ ). The purpose of this experiment was twofold: first, to verify Eq. (1.2) for the temperature dependence of the structure factor, specifically at  $k=k_p$ , where  $S(k)$  has its first and highest peak; and second, taking  $2k_F \approx k_p$ , to compare the temperature dependence of  $S(k_p)$  with that of  $\rho$  [given by Eq. (1.1)], which has been measured previously in these Nb-Ni glasses.<sup>8</sup> To date, very little has been done<sup>16</sup> to investigate the temperature dependence of  $S(k)$  of metallic glasses or to relate the results of such investigations in a detailed, systematic manner to the temperature variation of  $\rho$  in these materials. Our work represents the first investigation of  $S_T(k)$  over such a wide range of temperatures and compositions, as well as a direct test of the validity of Ziman's theory in the case of metallic glasses.

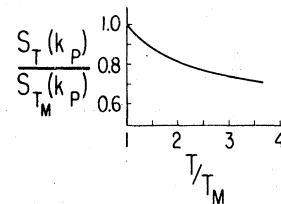


FIG. 1. Ratio, for liquid metals, of the value of  $S(k_p)$  at temperature  $T$  to its value close to the melting point  $T_M$ , plotted as a function of the reduced temperature. This is the universal curve found by Wagner (Ref. 17) in his study of the four liquid metals, Ga, Sn, Cd, and Zn.

Metallic glasses are of interest because they offer us an opportunity to probe structurally disordered metallic systems in the solid phase, i.e., at temperatures lower than those at which such systems have been available heretofore. Liquid metals, pure or alloyed, also have disordered structures, but cannot be observed at low temperatures. These have been many investigations, by x-ray or neutron diffraction, of the temperature dependence of the structure factor of liquid metals. Wagner<sup>17</sup> has found that Zn, Cd, Sn, and Ga all show a decrease in the height and a general broadening of the first peak of  $S(k)$  with increasing temperature. He finds that the variation of  $S(k_p)$  with temperature for all these metals follows a universal behavior, as shown in Fig. 1. Using the results of such measurements and Ziman's theory of electrical resistivity, the temperature coefficients of resistivity ( $\beta$ ) have been calculated for these liquid metals and were found to agree reasonably well (within 50%) with the measured values of  $\beta$ . We will compare the results we found for the metallic glasses with those found for the metallic liquids.

Another reason why the results of the experiment described here are of interest relates to a theory<sup>18</sup> of glass formation in metallic alloys. According to this model, one effect of alloying is to alter the effective valence so that  $2k_F$  changes in relation to  $k_p$ . When  $2k_F \approx k_p$ , a minimum is produced in the density of electronic states at the Fermi surface which makes the system stable against any perturbation of the spherically symmetric  $S(k)$  due to the development of long-range order, i.e., stable against crystallization. The stability of the glass structure is thus dependent on the position of the minimum in the electronic density of states through the condition  $2k_F \approx k_p$ , which is also assumed in applying Ziman's theory of resistivity to a metallic glass with a negative value of  $\beta$ . This assumption can thus be tested by checking whether  $S(k_p)$  has the same variation with temperature as does the

resistivity  $\rho$  which, according to Eq. (1.1), is proportional to  $S(2k_F)$ .

The paper is arranged as follows: In Sec. II we give details of the experimental setup and describe how the radial distribution function was calculated from the observed x-ray count rate as a function of the scattering angle. In Sec. III the results are presented and compared with the theory of temperature variation of  $S(k)$  mentioned earlier. The results are then used to predict the temperature dependence of  $\rho$  on the basis of Ziman's theory and the predictions are compared with the results of experiments on  $\rho$  of these samples. Section IV discusses the validity of Ziman's theory of resistivity in the context of the present work.

## II. EXPERIMENTAL

### A. X-ray diffraction arrangement

The samples used in this experiment were quenched amorphous alloys of Nb and Ni of compositions  $\text{Nb}_{0.4}\text{Ni}_{0.6}$  and  $\text{Nb}_{0.5}\text{Ni}_{0.5}$ . A study of a third sample,  $\text{Nb}_{0.6}\text{Ni}_{0.4}$ , was reported elsewhere.<sup>19</sup> These three compositions span almost the entire range of glass formation of these two metals. The samples were prepared by rapid arc furnace quenching of the melt.<sup>20</sup> Above room temperature the samples were mounted directly on the tip of a thermocouple in a Picker x-ray diffractometer. Mo  $K\alpha$  radiation was used for the diffraction experiments. The sample temperature was raised by blowing heated nitrogen gas over it; the temperature was stable to within  $\pm 5$  K. For measurements below room temperature the sample was placed in a LT-3-110 Heli-Tran cryostat and the temperature was regulated to within  $\pm 5$  K in the range from 4 to 300 K with a model 3610-A temperature Controller. Both instruments were manufactured by Air Products and Chemicals, Inc. The sample was surrounded by a vacuum shroud with 250- $\mu\text{m}$  Mylar windows to allow passage of the x rays.

The x-ray diffraction profiles were taken in transmission on a Syntex diffractometer. At the first peak  $k_p$  of  $\text{Nb}_{0.5}\text{Ni}_{0.5}$  the count rate was 700/s. In order to be able to calculate the radial distribution function (RDF) the room-temperature profiles of  $\text{Nb}_{0.5}\text{Ni}_{0.5}$  and  $\text{Nb}_{0.4}\text{Ni}_{0.6}$  were scanned between scattering angles  $2\theta = 3^\circ$  and  $120^\circ$  at intervals of approximately  $0.2^\circ$ , with 100 s of data collection at each point. To obtain good statistics in the measurement of  $S(k_p)$  as a function of temperature the region around the first peak at  $k_p$  was scanned in finer steps of  $0.04^\circ$  and a total of  $10^6$  counts were collected at the peak at each temperature at intervals of 50 K from 4 K (liquid-helium temperature) up to about 675 K, where the samples began to crystallize. This number of counts enabled us

to determine  $S_T(k_p)$  to within 0.1%. The major source of error was not the statistics but the stability of the x-ray source over long periods of time. It was also observed that the scattering angle corresponding to the position of the first peak for the  $\text{Nb}_{0.4}\text{Ni}_{0.6}$  sample shifted from  $19.26^\circ$  at room temperature (300 K) to  $19.19^\circ$  at 625 K. This corresponds to a decrease in  $k_p$  from 2.961 to 2.950  $\text{\AA}^{-1}$ . Assuming  $k_p \propto V^{-1/3}$ , where  $V$  is the volume of the sample, one can calculate the thermal coefficient of linear expansion from the relation  $\alpha = (\Delta k_p/k_p)\Delta T$ .  $\alpha$  was calculated to be  $\sim 1.0 \times 10^{-5} \text{ K}^{-1}$ , which compares well with the value calculated<sup>19</sup> for the  $\text{Nb}_{0.6}\text{Ni}_{0.4}$  sample. This shift in the position of  $S_T(k_p)$  was tracked carefully and x-ray counts for  $S_T(k_p)$  at each temperature were collected at the value of  $2\theta$  corresponding to the correct position for the peak. Below room temperature the thermal expansion of the sample became very small and it was not necessary to vary  $2\theta$  with temperature. The data from the high- and low-temperature runs were matched at room temperature, which was the common point in these two temperature ranges. The second peak of  $\text{Nb}_{0.4}\text{Ni}_{0.6}$  was similarly scanned every 50 K from room temperature up to 550 K. During the high-temperature measurements the samples were cycled back to room temperature several times to ensure that the x-ray source was stable and that no irreversible structural changes had occurred in the sample.

In order to gain intensity sufficient to enable an accurate determination of  $S_T(k_p)$ , the angular resolution of the spectrometer had to be reduced from the value used to record the full  $S(k)$  data for the RDF analyses ( $\sim \frac{1}{2}^\circ$ ) to approximately  $2^\circ$ . This introduced a small systematic error in the measurement of the temperature dependence of the structure factor. We can correct for this effect in two ways. (i) We measured the room temperature  $S(k)$  with both good resolution and the low resolution needed to obtain the temperature dependence of  $S(k)$ , and found a 10% difference between the two values of  $S(k_p)$  so obtained. Using Eq. (1.2), we calculate that this difference leads to a 14% change in the slope of  $S(k_p)$  vs  $T$ . (ii) We also measured  $S_T(k_p)$  for one sample with good resolution over a more limited range of temperature (300–500 K) and found an increase in the slope of 13%, in good agreement with the calculation.

### B. Analysis of room-temperature x-ray spectra

Before being normalized to electron units, the measured x-ray intensities had to be corrected for the absorption in the sample, the experimentally measured background due to air scattering, and the polarization effects of the monochromator.

A unified method of doing this has been developed by Ergun *et al.*<sup>21</sup> and was used by us with certain modifications. For the symmetrical-transmission geometry used in this experiment the following quantities were calculated:

$$\Phi(k, \mu t) = \frac{I(k)P(k)}{\left[\sum_p f_p^2(k)\right] \exp(-\mu t \cos \theta) \sec \theta}, \quad (2.1)$$

$$g(k, \mu t) = \frac{\sum_p C_p(k) \{1 - \exp[-[B(k) - 1] \mu t \sec \theta]\}}{\sum_p f_p^2(k) [B(k) - 1] \mu t \sec \theta},$$

where  $I(k)$  is the measured intensity, minus air scattering, at the wave vector  $k = 4\pi \sin \theta / \lambda$ ,  $2\theta$  is the scattering angle, and  $\lambda$  is the wavelength of the radiation ( $\lambda = 0.71 \text{ \AA}$  for Mo  $K\alpha$  radiation),  $P(k)$  is the polarization correction factor,  $B(k)$  the relativistic Breit-Dirac correction to Compton scattering,  $\mu$  the linear-absorption coefficient,  $t$  the thickness of the sample, and  $\sum_p C_p(k)$  and  $\sum_p f_p^2(k)$  are respectively the weighted sums over the different atomic species in the sample of the Compton (or incoherent) and coherent atomic scattering factors (expressed in electron units). The structure factor  $S(k)$  is obtained from:

$$\Phi(k, \mu t) = D[g(k, \mu t) + 1] + Di(k), \quad (2.2)$$

where  $D$  is the normalization factor for converting the measured intensities into electron units and  $i(k) = S(k) - 1$  is the interference function that oscillates around zero. For each value of  $\mu t$ ,  $\Phi(k)$  is plotted against  $g(k)$  and a best-fit straight line is drawn through the data points. The method is to vary  $\mu t$  until the straight line has equal slope and intercept (each equal to  $D$ ). In obtaining the best-fit straight line, we modified the procedure of Ergun *et al.*<sup>21</sup> by introducing two necessary criteria to be satisfied by that line. Since the data points differ from the line due to the term  $Di(k)$ , we employ the sum rule satisfied by the static structure factor:

$$\int_0^\infty [S(k) - 1] k^2 dk = \int_0^\infty i(k) k^2 dk = 0. \quad (2.3)$$

In practice, the upper and lower limits in the integral were replaced by  $k_{\max}$  and  $k_{\min}$ , that is, the points in  $k$  space between which the data were collected. The other condition was that of a modified least squares, whereby the deviation of each point from the fitted straight line was weighted by the corresponding  $k^2$  and the sum total of weighted deviations was made a minimum. The reason for imposing this condition was that the oscillations of  $i(k)$  around zero are small for large  $k$ . Hence the desired linear correlation between  $\Phi$  and  $g$  should be more accurately determined from the data points at large  $k$  than from those at small  $k$ , where the

oscillations in  $i(k)$  are large and where the background corrections are relatively uncertain.

These two conditions uniquely specify the straight line to be drawn through the data for each value of  $\mu t$ . This analysis gives the value of  $\mu t$  and the slope  $D$  of the line with equal slope and intercept, which in turn yielded the structure factor from Eq. (2.2). The radial distribution function (RDF) can then be expressed by relation<sup>22</sup>

$$4\pi r^2 n(r) = 4\pi r^2 n_0 + \frac{2r}{\pi} \int_0^\infty dk [S(k) - 1] k \sin kr, \quad (2.4)$$

where  $n_0$  is the mean atomic density of the sample.

The area under the first peak of the RDF, that is, the integral of the function  $4\pi r^2 n(r)$  between zero and the first minimum, gives the mean nearest-neighbor coordination number. This number was calculated from the RDF curves for the samples  $\text{Nb}_{0.5}\text{Ni}_{0.5}$  and  $\text{Nb}_{0.4}\text{Ni}_{0.6}$ .

### III. RESULTS

#### A. $S(k)$ and RDF at room temperature

Figure 2 shows the structure factor  $S(k)$  for the glass compositions  $\text{Nb}_{0.4}\text{Ni}_{0.6}$  and  $\text{Nb}_{0.5}\text{Ni}_{0.5}$ , obtained by the method outlined in Sec. II. For each,  $S(k)$  has a slightly asymmetric sharp first peak, while the second peak has a shoulder on its high-angle side. The subsequent peaks become smaller and for large values of  $k$  only weak modulations about the horizontal line  $S(k) = 1$  are observed. The maximum value and the positions of the first few peaks of  $S(k)$  are given in Table I.

Figure 3 shows the computed RDF curves for the two samples. Each curve oscillates about the average-density curve  $4\pi r^2 n_0$ . The value<sup>22</sup> of  $n_0$  was taken

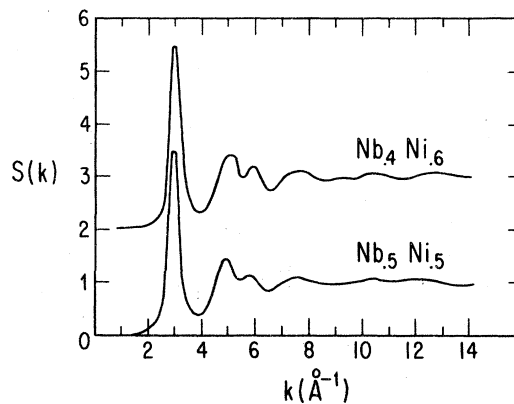


FIG. 2. Structure factor of the two Nb-Ni samples,  $\text{Nb}_{0.5}\text{Ni}_{0.5}$  and  $\text{Nb}_{0.4}\text{Ni}_{0.6}$ . The curve for the second sample has been displaced vertically by +2.

TABLE I. Structure results for amorphous Nb-Ni alloys.

Alloy composition	$S(k_p)$	$k_p$ ( $\text{\AA}^{-1}$ )	Positions of maxima <sup>a</sup> in $S(k)$			RDF			Mean coordination number
			$k_{2p}$ ( $\text{\AA}^{-1}$ )	$k'_{2p}$ ( $\text{\AA}^{-1}$ )	$r_1$ ( $\text{\AA}$ )	$r_2$ ( $\text{\AA}$ )	$r'_2$ ( $\text{\AA}$ )	$k_p r_1$	
Nb <sub>0.5</sub> Ni <sub>0.5</sub>	3.49	2.94	4.89	5.79	2.74	4.62	5.41	8.06	13.5
Nb <sub>0.4</sub> Ni <sub>0.6</sub>	3.49	3.00	5.03	5.92	2.65	4.54	5.44	7.95	13.5

<sup>a</sup> $k'_{2p}$  and  $r'_2$  denote the positions of the subsidiary maxima associated with the second peaks of  $S(k)$  and RDF, respectively.

to be 2% less than the weighted average of the atomic densities for Nb and Ni. Table I also shows the positions of the first few maxima in the RDF's and the mean coordination number obtained from these RDF curves. These coordination numbers are larger than 12 for both samples, which implies that the alloy structure is close-packed and remains so over the composition range spanned by these samples.

It is interesting to note the similarities between some qualitative and quantitative features of the results on  $S(k)$  and RDF for Nb-Ni glasses and similar results reported for other amorphous alloys such as Fe-P-C,<sup>23</sup> Pd-Ni-P,<sup>24</sup> and Pd-Fe-P.<sup>24</sup> For example, the shoulder on the high-angle side of the second peak of  $S(k)$  and a double peak beyond the first maximum of the RDF are features common to the structural data on all these alloys.

The data in Table I for the Nb-Ni glasses show that (a) the ratio of the second to the first nearest-neighbor distance,  $r_2/r_1$  is about 1.7 (in most<sup>25</sup> liquid metals the value for this ratio is 1.85);

(b) the positions of the first peaks in  $S(k)$  and RDF satisfy the relation  $k_p r_1 \approx \text{const}$  ( $\sim 8.0$ ). This value is close to that given by the Ehrenfest relation<sup>25</sup> for a close-packed hard-sphere system (7.72). Both these quantitative observations are also in agreement with the findings from the other alloys mentioned above. On the other hand, the x-ray scattering data on amorphous Ni-Pt-P samples<sup>26</sup> over a wide range of compositions show no subsidiary maxima associated with the second peak of  $S(k)$  or the RDF, whereas the ratio  $r_2/r_1$  is  $\sim 1.86$  and the product  $k_p r_1$  varies between 7.5 and 8.0 with the composition of the alloy. Such results indicate a difference in the microscopic structures, i.e., short-range order, of these two groups of amorphous alloys.

#### B. Temperature dependence of structure factor and resistivity of glasses

The calculated temperature dependence of the structure factor in an amorphous solid is given in Eq. (1.2), where  $S_T(k)$  is expressed in terms of its value at zero temperature and the Debye-Waller factor  $e^{-W(T)}$ . In the Debye model of a solid, one has<sup>27</sup>

$$W(T) - W(0) = \frac{3\hbar^2 k^2}{2Mk_B\theta} \left(\frac{T}{\theta}\right)^2 \int_0^{\theta/T} \frac{z dz}{e^z - 1}, \quad (3.1)$$

where  $\theta$  is the Debye temperature,  $M$  is the atomic mass, and  $k_B$  is the Boltzmann constant.

In this experiment  $S_T(k_p)$  has been measured for temperatures from 4 to 675 K. One can compare the observed ratios  $S_T(k_p)/S_0(k_p)$  with the ones calculated from Eq. (1.2), using the values of the integral in Eq. (3.1) tabulated by Zener.<sup>28</sup> In doing this we must emphasize that there is only one parameter  $\theta$  which may be adjusted to fit the prediction of Eqs. (1.2) and (3.1) to the data.

Figure 4 shows the ratio  $S_T(k_p)/S_0(k_p)$  for the two samples of Nb-Ni plotted against the temperature. The data have been corrected for the finite resolution of the spectrometer. Also included in this figure are the high-temperature data, which were reported earlier,<sup>19</sup> on a third composition Nb<sub>0.6</sub>Ni<sub>0.4</sub>. The solid lines represent the fit of Eq. (1.2) to the data with the value of  $\theta$  indicated in

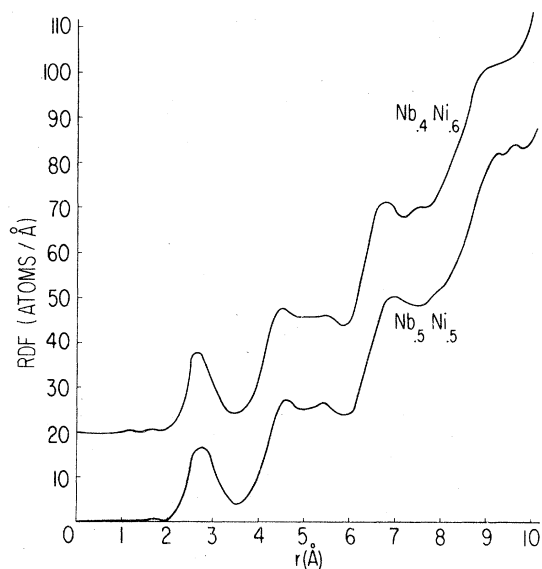


FIG. 3. Radial distribution function for the two Nb-Ni samples, obtained from the structure factors shown in Fig. 2. The curve for the Nb<sub>0.4</sub>Ni<sub>0.6</sub> sample has been displaced vertically by +20.

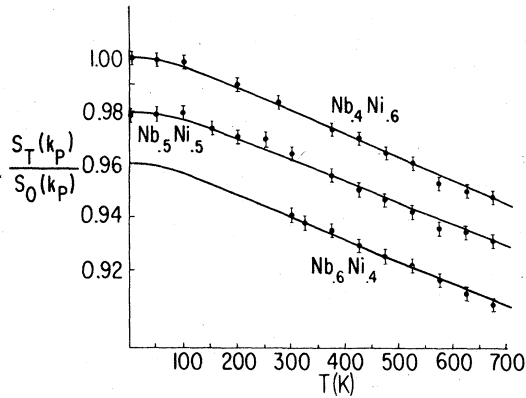


FIG. 4. Ratio of the value of  $S(k_p)$  at temperature  $T$  to its value at  $T=0$  for the three Nb-Ni samples. The solid lines represent the predictions of Eqs. (1.2) and (3.1), with only one adjustable parameter,  $\theta$ . The values  $\theta$  used are given in Table II. The data points shown have already been corrected for the finite resolution of the spectrometer, as discussed in the text.

Table II. As one can see, the fit is excellent.

By our analysis of the temperature dependence of the first peak we have determined the one adjustable parameter in the theory,  $\theta$ . The prediction for the temperature dependence of the structure factor at any other value of  $k$  is now completely determined. We have, for the  $\text{Nb}_{0.4}\text{Ni}_{0.6}$  sample, measured the temperature dependence of the height of the second peak in the structure factor. In Fig. 5 we show the results, along with the prediction of the theory. The agreement between data and theory (with no adjustable parameters left) is excellent. This helps confirm the quadratic dependence on  $k$  of the Debye-Waller factor [Eq. (3.1)], as well as the dependence of  $S_T(k)$  on the value of  $S_0(k) - 1$  in Eq. (1.2). Of perhaps more importance is that this result on the second peak indicates that the assumptions which were made in deriving Eq. (1.2), specifically the use of one average Debye temperature for all the peaks in  $S(k)$ , were physically justified.

As mentioned above, a principal motivation behind this investigation of the  $T$  dependence of  $S(k)$  is the attempt at explaining the behavior of the resistivity of metallic glasses as a function of  $T$ . Figure 6 shows the resistivity of Nb-Ni glasses as a function of  $T$  from 4 to 340 K, as was reported in an earlier paper.<sup>8</sup> From Eq. (1.1) we obtain

$$\frac{1}{\rho} \frac{\Delta \rho}{\Delta T} \sim \frac{1}{S(2k_F)} \frac{\Delta S(2k_F)}{\Delta T} \quad (3.2)$$

if  $E_F$ ,  $k_F$ ,  $\Omega$ , and  $\eta_2(E_F)$  are assumed to be approximately temperature independent. Taking  $2k_F \approx k_p$ , we can calculate the right-hand side of Eq. (3.2) from the present data and compare it with the measured  $\beta \equiv (1/\rho)\Delta\rho/\Delta T$ . This is done by (a) considering the *entire* temperature range spanned by the resistivity data in Fig. 6 and (b) considering only the portion of the resistivity curves between 300 and 340 K, where the curves start flattening out. The calculated values of the two sides of Eq. (3.4) are presented in Table II. It will be seen that the temperature variation of  $S(k_p)$  is large enough to explain the resistivity variation above room temperature, but falls short by 27% when one considers the entire range of the resistivity data. The high-temperature resistivity has been measured<sup>1</sup> up to 875 K for the sample  $\text{Nb}_{0.4}\text{Ni}_{0.6}$ , and has been found to decrease linearly in the range from 300 to 800 K at a rate given by  $\beta = 5 \times 10^{-5} \text{ K}^{-1}$ , which is smaller than the slope of the linearly decreasing  $[S_T(k_p)/S_0(k_p)]$  vs  $T$  curve for  $\text{Nb}_{0.4}\text{Ni}_{0.6}$  in this temperature region.

It is also of interest to compare the values of the Debye temperature  $\theta$  used to fit the low-temperature-resistivity<sup>8</sup> data and the structure-factor data. A comparison of the Debye temperatures in Table II shows that the resistivity data imply a 30% smaller value of  $\theta$  than do the  $S(k)$  data. One can observe that the values of  $\theta$  we derive from the x-ray data are very close to the average value of  $\theta$ , weighted by their concentrations in the alloy, of the two pure elements. This value,  $\theta_{av}$ , is given in the last column in Table II.

TABLE II. Comparison of resistivity and structure-factor data.

Alloy composition	$\frac{1}{\rho} \frac{\Delta \rho}{\Delta T}$ for		$\frac{1}{S(k_p)} \frac{\Delta S(k_p)}{\Delta T}$ for		$\theta_p$ (K) <sup>a</sup>	$\theta_s$ (K) <sup>a</sup>	$\theta_{av}$ (K) <sup>a</sup>
	$T=4 \text{ K} \rightarrow 340 \text{ K}$ (K <sup>-1</sup> )	$T=300 \text{ K} \rightarrow 340 \text{ K}$ (K <sup>-1</sup> )	$T=4 \text{ K} \rightarrow 675 \text{ K}$ (K <sup>-1</sup> )	$T=300 \text{ K} \rightarrow 675 \text{ K}$ (K <sup>-1</sup> )			
$\text{Nb}_{0.4}\text{Ni}_{0.6}$	$-11.1 \times 10^{-5}$	$-7.0 \times 10^{-5}$	$-8.1 \times 10^{-5}$	$-9.0 \times 10^{-5}$	$248 \pm 5$	$370 \pm 10$	380
$\text{Nb}_{0.5}\text{Ni}_{0.5}$	$-10.0 \times 10^{-5}$	$-7.0 \times 10^{-5}$	$-7.2 \times 10^{-5}$	$-7.9 \times 10^{-5}$	$248 \pm 5$	$370 \pm 10$	363
$\text{Nb}_{0.6}\text{Ni}_{0.4}$	$-8.4 \times 10^{-5}$	$-7.0 \times 10^{-5}$	...	$-8.9 \times 10^{-5}$	$248 \pm 5$	$340 \pm 10$	345

<sup>a</sup> $\theta_p$  and  $\theta_s$  are the Debye temperatures obtained from the resistivity and structure-factor data, respectively.  $\theta_{av}$  is the value of the Debye temperature found by averaging the values of  $\theta$ , weighted by their concentration in the alloy, of the two pure elements [ $\theta$  (Ni)=450 K and  $\theta$  (Nb)=275 K]. Values of  $\theta$  for the pure elements are taken from C. Kittel, *Introduction to Solid State Physics*, 5th Ed., (Wiley, New York, 1976) p. 126.

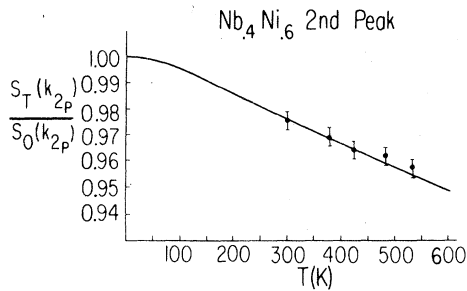


FIG. 5. Ratio of the value of  $S(k_p)$  at temperature  $T$  to its value at  $T=0$  for the  $\text{Nb}_{0.4}\text{Ni}_{0.6}$  sample. The solid line represents the prediction of Eqs. (1.2) and (3.1), with no adjustable parameters. The value of  $\theta$  has already been determined by the data taken at the first peak.

#### IV. DISCUSSION

The results on the temperature dependence of the structure factor of metallic glasses presented in this paper agree well with some qualitative features observed in similar measurements on liquid metals: the height of the first peak of  $S(k)$  decreases and the peak itself broadens as the temperature is increased. Wagner<sup>17</sup> has plotted the experimentally observed ratio  $S_T(k_p)/S_{T_M}(k_p)$  against  $T/T_M$  for the four liquid metals Sn, Ga, Cd, and Zn, where  $T_M$  is the melting point of the metal. He found that a universal curve could be drawn through all the experimental points, as shown in Fig. 1. The behavior of the data for glasses shown in Fig. 4 is markedly different from that for the liquids. The curve is linear over

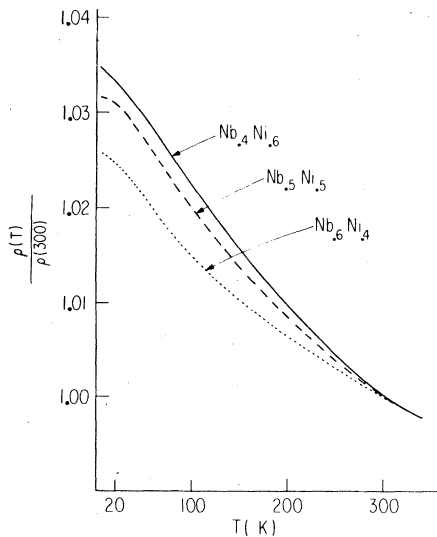


FIG. 6. Resistivity as a function of temperature for the three Nb-Ni samples. The resistivity is normalized to its value at room temperature. The data are taken from Ref. 8.

most of the temperature range, becoming constant at the lowest temperatures. In the liquid, however,  $S(k_p)$  drops fastest at the lowest temperatures and begins to flatten out at high temperatures. These results suggest a qualitative difference in the temperature dependence of the structure factor in the liquid and the glassy states.

The measured temperature dependence of the intensity at the first peak,  $S_T(k_p)$ , agrees well with the theory represented by Eq. (1.1). The fitting was done with only a single adjustable parameter, namely the Debye temperature  $\theta$  for the alloy. The temperature dependence of the intensity of the second peak for the  $\text{Nb}_{0.4}\text{Ni}_{0.6}$  sample also agrees with the prediction of the theory as given by Eq. (3.4). This serves as a further confirmation of the theory. It has been proposed<sup>13</sup> that a negative temperature coefficient of resistivity, as observed in Nb-Ni glasses, may be related on the basis of Ziman's theory, to the decrease of  $S(k_p)$  with increasing temperature. Above room temperature the magnitude of this decrease is about 30% larger than the magnitude of the decrease of the resistivity, while below room temperature the resistivity decreases faster than the structure factor. Using Ziman's theory, Knoll<sup>29</sup> has found from an analysis of the temperature-dependent structure-factor data on liquid Zn a negative temperature coefficient of resistivity which is 25% less than the experimentally measured value. From a similar analysis for the liquid metals Zn, Cd, Sn, and Ga Wagner has found<sup>17</sup> temperature coefficients of resistivity in fair agreement with the observed values.

There has not been any direct measurement of the temperature dependence of  $S(k_p)$  for liquid alloys (as distinct from pure metals). Güntherodt *et al.*<sup>30</sup> have speculated that the different temperature coefficients of the resistivity in the glassy and liquid alloys of  $\text{Pb}_{81}\text{Si}_{19}$  are due to a different temperature dependence of  $S(k)$  in these two states. The results presented earlier in this section on the behavior of the structure factor in different liquid metals and glassy alloys of varying compositions seems to corroborate this idea.

In comparing our results for  $S_T(k_p)$  with the resistivity data we have tacitly assumed that  $2k_F \approx k_p$  for the alloy concentrations. In a real binary alloy three partial structure factors are necessary to describe the scattering of both x rays and electrons. The resistivity in this case has the following form<sup>11</sup>:

$$\rho = C(E_F) \int_0^{2k_F} |u(k)|^2 k^3 dk, \quad (4.1)$$

where

$$|u(k)|^2 = c_A |t_A|^2 (1 - c_A + c_A S_{AA}) + c_B |t_B|^2 \times (1 - c_B + c_B S_{BB}) + c_A c_B (t_A^* t_B + t_A t_B^*) (S_{AB} - 1), \quad (4.2)$$

and where  $C(E_F)$  is a factor containing a function of  $E_F$ ;  $c_A$  and  $c_B$  are the concentrations of elements A and B;  $t_A$  and  $t_B$  are the single-site  $t$  matrices for scattering of electrons from the two types of atoms, and  $S_{AA}$ ,  $S_{AB}$ , and  $S_{BB}$  are the partial structure factors of the alloy. The expression for the resistivity given in Eq. (1.1) is obtained by assuming that (a) the three partial structure factors can be replaced by a single structure factor (b)  $|t_A| = |t_B|$ , each being proportional to  $\sin[\eta_2(E_F)]$ , and that (c) the integral in Eq. (4.1) can be replaced by the value of the integrand at the upper limit,  $k = 2k_F$ . The x-ray diffraction provides only a weighted average of the three partial structure factors. In order to yield a negative value for the temperature coefficient of resistance  $\beta$ ,  $2k_F$  may be near the peak of any one of these three structure factors. The value of  $|\beta|$  can therefore be larger than that expected from our x-ray measurements if one of the partials has a significantly larger temperature variation than the average value measured by x rays [which weights strongly the structure factor  $S_{\text{Nb,Ni}}(k)$ ]. By setting  $2k_F$  near the peak of the x ray  $S(k)$  we only obtain an estimate of how large  $(1/\rho)d\rho/dT$  can be. For a more accurate calculation one should extract all three structure factors, by performing three different scattering experiments, and compute the integral in Eq. (4.1). We are presently involved in combining neutron scattering experiments with our x-ray studies in order to get additional information about the temperature dependence of the various partial structure factors in another amorphous alloy.

Besides making the above approximations, we have also neglected the temperature dependences of  $k_F$ ,  $E_F$ , and  $\eta_2(E_F)$  in calculating  $\beta$  from Eq.

(1.1). Inclusion of these additional sources of temperature dependence may improve the agreement between our experimental results and the predictions of the Ziman theory. However, it is not at all clear according to this theory whether the magnitude of  $\beta$  should be larger at low temperatures than at high temperatures, as is found experimentally. Various possibilities may be considered to explain this observation: (a) there could be additional high-temperature scattering, perhaps electron-electron scattering;<sup>8</sup> (b) the long-wavelength phonons could become ineffective at scattering electrons;<sup>31</sup> and (c) there could be additional scattering at low temperatures, perhaps caused by electrons scattering from the two-level tunneling states mentioned earlier.<sup>4,5,6</sup> The measurements reported here cannot distinguish between these possibilities.

However, the extent of agreement we find in the glasses between the temperature dependence of the structure factor and the temperature dependence of the resistivity is very similar to that found in the liquid metals. Although the variation with temperature of the structure factor is somewhat smaller than that of the resistivity, the discrepancy is not very great. In our calculations we have made a number of simplifying assumptions which may have underestimated the predicted value of  $\beta$ .

#### ACKNOWLEDGMENTS

We are grateful to Professor B. C. Giessen for providing the samples and to Professor H. Fritzche for the loan of his Heli-Tran cryostat. We would also like to thank Dr. J. Pluth for technical assistance and Professor S. Solin for stimulating conversations. This work was supported by NSF Grant No. DMR 77-09931 and the NSF-MRL program. One of us (R.C.) was supported by an IBM-James Franck Fellowship.

<sup>1</sup>For example, see the review article by H. -J. Güntherodt, *Adv. Solid State Phys.* **17**, 25 (1977).

<sup>2</sup>S. R. Nagel, *Phys. Rev. Lett.* **41**, 990 (1978).

<sup>3</sup>A. K. Sinha, *Phys. Rev. B* **1**, 4541 (1970).

<sup>4</sup>R. W. Cochrane, R. Harris, J. O. Strom-Olson, and M. J. Zuckermann, *Phys. Rev. Lett.* **35**, 676 (1975); R. W. Cochrane and J. O. Strom-Olson, *J. Phys. F* **7**, 1799 (1977).

<sup>5</sup>C. C. Tsuei, *Solid State Commun.* **27**, 691 (1978).

<sup>6</sup>J. L. Black and B. L. Gyorffy, *J. Phys. (Paris)* **39**, C6-941 (1978); J. L. Black, B. L. Gyorffy, and J. Jäckle (unpublished).

<sup>7</sup>P. W. Anderson, B. I. Halperin, and C. M. Varma, *Philos. Mag.* **25**, 1 (1972); W. A. Phillips, *J. Low Temp. Phys.* **7**, 351 (1972).

<sup>8</sup>S. R. Nagel, J. Vassiliou, P. M. Horn, and B. C. Giessen, *Phys. Rev. B* **17**, 462 (1978).

<sup>9</sup>N. F. Mott, *Philos. Mag.* **26**, 1249 (1972).

<sup>10</sup>F. R. Sofran, G. R. Gruzalski, J. W. Weymouth, P. J. Sellmyer, and B. C. Giessen, *Phys. Rev. B* **14**, 2160 (1976).

<sup>11</sup>J. M. Ziman, *Philos. Mag.* **6**, 1013 (1961); for a review of the Ziman theory as applied to liquid metals see G. Busch and H. -J. Güntherodt, in *Solid State Physics*, edited by H. Ehrenreich, F. Seitz, and D. Turnbull (Academic, New York, 1975), Vol. 29, p. 235.

<sup>12</sup>R. Evans, D. A. Greenwood, and P. Lloyd, *Phys. Lett.* **35A**, 57 (1971).

<sup>13</sup>S. R. Nagel, *Phys. Rev. B* **16**, 1694 (1977).

<sup>14</sup>P. J. Cote and L. V. Meisel, *Phys. Rev. Lett.* **39**, 102



- (1977); K. Frobose and J. Jäckle, *J. Phys. F* **7**, 2331 (1977); *ibid* (to be published).
- <sup>15</sup>R. Kaplow, T. A. Rowe, and B. L. Averbach, *Phys. Rev.* **168**, 1068 (1968).
- <sup>16</sup>P. J. Cote, G. P. Capsinalis, and L. V. Meisel, *Phys. Rev. B* **16**, 4651 (1977); Y. Waseda, *Bull. Am. Phys. Soc.* **23**, 467 (1978).
- <sup>17</sup>C. N. J. Wagner, in *Liquid Metals 1976*, Conference Series No. 30, edited by R. Evans and D. A. Greenwood (Institute of Physics, Bristol and London, 1976), p. 110.
- <sup>18</sup>S. R. Nagel and J. Tauc, *Phys. Rev. Lett.* **35**, 380 (1975); Ref. 17, p. 283.
- <sup>19</sup>R. Clarke and S. R. Nagel, *Solid State Commun.* **27**, 215 (1978).
- <sup>20</sup>M. Ohring and A. Haldipur, *Rev. Sci. Instrum.* **42**, 530 (1971).
- <sup>21</sup>Sabri Ergun, James Bayer, and Wayne Van Buren, *J. Appl. Phys.* **38**, 3540 (1967).
- <sup>22</sup>We have adopted here the standard definition of the radial distribution function as found in the literature; see, for example, G. S. Cargill III, in *Solid State Physics*, edited by H. Ehrenreich, F. Seitz, and D. Turnbull (Academic, New York, 1975), Vol. 30, p. 227.
- <sup>23</sup>S. C. H. Lin and P. Duwez, *Phys. Status Solidi* **34**, 469 (1969).
- <sup>24</sup>P. Maitrepierre, *J. Appl. Phys.* **40**, 4826 (1969).
- <sup>25</sup>B. C. Giessen and C. N. J. Wagner, in *Physics and Chemistry of Liquid Metals*, edited by S. Z. Beer (Dekker, New York, 1972), p. 633.
- <sup>26</sup>A. K. Sinha and P. Duwez, *J. Phys. Chem. Solids* **32**, 267 (1971).
- <sup>27</sup>See, for example, J. Ziman, *Principles of the Theory of Solids* (Cambridge University, Cambridge, England, 1969), Chap. 2.
- <sup>28</sup>C. Zener, *Phys. Rev.* **49**, 122 (1936).
- <sup>29</sup>W. Knoll, Ref. 15, p. 117.
- <sup>30</sup>H. -J. Güntherodt, H. U. Kunzi, M. Liard, R. Muller, R. Oberle, and H. Rudin, Ref. 16, p. 342.
- <sup>31</sup>P. J. Cote and L. V. Meisel, *Phys. Rev. Lett.* **40**, 1586 (1978).